

Inverse design and fabrication tolerances of ultra-flattened dispersion holey fibers

F. Poletti, V. Finazzi, T. M. Monro, N. G. R. Broderick, V. Tse
and D. J. Richardson

Optoelectronic Research Centre, University of Southampton, SO17 1BJ, UK
frap@orc.soton.ac.uk

Abstract: We employ a Genetic Algorithm for the dispersion optimization of a range of holey fibers (HF) with a small number of air holes but good confinement loss. We demonstrate that a dispersion of 0 ± 0.1 ps/nm/km in the wavelength range between 1.5 and $1.6 \mu\text{m}$ is achievable for HFs with a range of different transversal structures, and discuss some of the trade-offs in terms of dispersion slope, nonlinearity and confinement loss. We then analyze the sensitivity of the total dispersion to small variations from the optimal value of specific structural parameters, and estimate the fabrication accuracy required for the reliable fabrication of such fibers.

© 2005 Optical Society of America

OCIS codes: (060.4370) Nonlinear optics, fibers; (060.2280) Fiber design and fabrication; (060.2430) Fibers, single mode; (060.2330) Fiber optics communications

References and links

1. T. Okuno, M. Hirano, T. Kato, M. Shigematsu and M. Onishi, "Highly nonlinear and perfectly dispersion-flattened fibers for efficient optical signal processing applications," *Electronics Letters* **39**, 972-974 (2003).
2. T. M. Monro, D. J. Richardson, N. G. R. Broderick and P. J. Bennett, "Holey optical fibers: an efficient modal model," *J. Lightwave Technol.* **17**, 1093-1102, (1999).
3. A. Ferrando, E. Silvestre and P. Andres, "Designing the properties of dispersion-flattened photonic crystal fibers," *Opt. Express* **9**, 687-697 (2001). <http://www.opticsexpress.org/abstract.cfm?URI=OPEX-9-13-687>
4. W. H. Reeves, J. C. Knight, P. St. J. Russell and P. J. Roberts "Demonstration of ultra-flattened dispersion in photonic crystal fibers," *Opt. Express* **10**, 609-613 (2002).
<http://www.opticsexpress.org/abstract.cfm?URI=OPEX-10-14-609>
5. K. P. Hansen, "Dispersion flattened hybrid-core nonlinear photonic crystal fiber," *Opt. Express* **11**, 1503-1509 (2003). <http://www.opticsexpress.org/abstract.cfm?URI=OPEX-11-13-1503>
6. K. Saitoh, M. Koshiba, T. Hasegawa and E. Sasaoka, "Chromatic dispersion control in photonic crystal fibers: application to ultra-flattened dispersion," *Opt. Express* **11**, 843-852 (2003).
<http://www.opticsexpress.org/abstract.cfm?URI=OPEX-11-8-843>
7. F. Poli, A. Cucinotta, S. Selleri and A. H. Bouk, "Tailoring of flattened dispersion in highly nonlinear photonic crystal fibers," *IEEE Photon. Technol. Lett.* **16**, 1065-1067 (2004).
8. G. Renversez, B. Kuhlmeier and R. McPhaedran, "Dispersion Management with microstructured optical fibers: ultraflattened chromatic dispersion with low losses," *Opt. Lett.* **28**, 989-991 (2003).
9. T. Wu and C. Chao, "A novel ultra-flattened dispersion photonic crystal fiber," *IEEE Photon. Technol. Lett.* **17**, 67-69 (2005).
10. A. Cucinotta, S. Selleri, L. Vincetti and M. Zoboli, "Perturbation analysis of dispersion properties in photonic crystal fibers through the finite element method", *J. Lightwave Technol.* **20**, 1433-1441,(2002).
11. E. Kerrinckx, L. Bigot, M. Douay and Y. Quiquempois, "Photonic crystal fiber design by means of a genetic algorithm," *Opt. Express* **12**, 1990-1995 (2004). <http://www.opticsexpress.org/abstract.cfm?URI=OPEX-12-9-382>
12. T. P. Wite, B. T. Kuhlmeier, R. C. McPhaedran, D. Maystre, G. Renversez, C. M. de Sterke and L. C. Botten, "Multipole method for microstructured optical fibers. I. Formulation," *J. Opt. Soc. Am. B* **19**, 2322-2330 (2002).
13. D. E. Goldberg, *Genetic algorithms in search, optimization and machine learning*, (Addison-Wesley, New York, 1989).

14. J. Skaar and K. M. Risvik, "A genetic algorithm for the inverse problem in synthesis of fiber gratings," *J. Light-wave Technol.* **16**, 1928, (1998).
 15. H. Ebendorff-Heidepriem, P. Petropoulos, S. Asimakis, V. Finazzi, R. C. Moore, K. Frampton, F. Koizumi, D. J. Richardson, and T. M. Monro, "Bismuth glass holey fibers with high nonlinearity," *Opt. Express* **12**, 5082-5087 (2004). <http://www.opticsexpress.org/abstract.cfm?URI=OPEX-12-21-5082>
 16. K. M. Hilligse, T. V. Andersen, H. N. Paulsen, C. K. Nielsen, K. Mlmer, S. Keiding, R. Kristiansen, K. P. Hansen, and J. J. Larsen, "Supercontinuum generation in a photonic crystal fiber with two zero dispersion wavelengths," *Opt. Express* **12**, 1045-1054 (2004). <http://www.opticsexpress.org/abstract.cfm?URI=OPEX-12-6-1045>
-

1. Introduction

Nonlinear fiber based devices such as wavelength converters, parametric amplifiers, supercontinuum sources and switches are attractive candidates for application in future high-capacity, all-optical networks. In order to reduce the physical length and/or required operating powers, and to maximize the operating bandwidth of many such devices, it is generally desirable to use fibers with as high nonlinearity and low and flat a group velocity dispersion as is possible. As a result the development of dispersion-flattened, dispersion-shifted fibers with high nonlinearity has attracted considerable attention in recent years. Steady progress has been made and, by careful design and engineering of the refractive index profile, conventional doped fiber fabrication approaches have been used to produce fibers with dispersion slopes as low as of $0.0002 \text{ ps/nm}^2/\text{km}$ with nonlinear coefficients of $10 \text{ W}^{-1} \cdot \text{km}^{-1}$ [1] at wavelengths in the C-band. These figures represent the current state-of-the-art in terms of trade-off between dispersion flatness and nonlinearity per unit length for fibers with zero-dispersion wavelengths around 1550nm. It is to be appreciated that fibers with higher nonlinearity can be produced, but only by compromising the dispersion slope.

More recently Holey Fibers (HF) have emerged as a means to produce high nonlinearity fibers with unique dispersive properties. HF guide light in a solid core surrounded by air holes through a modified form of internal reflection. Their unusual properties result physically from the high index contrast between silica and air which allows for extremely tight optical confinement and a strongly wavelength dependent effective cladding index. This later feature provides the possibility of compensation of the material dispersion over extremely broad wavelength ranges [2, 3]. HF technology also provides for considerable design flexibility through control of the hole size (d) and pitch (Λ).

So far nonlinear dispersion flattened HF (NL-DFHF) have been experimentally realized using triangular lattice cladding structures with constant diameter holes. These fibers have comprised either a pure silica core and 11 rings of uniform sized holes with small d/Λ , [4], or a hybrid germanium doped triangular core and 12 rings of air holes [5]. A large number of ring layers is required in both instances to reduce the confinement losses to an acceptable level, and adds complexity to the fabrication process. It has been shown more recently in a number of theoretical papers that it should be possible to reduce the number of rings of air holes required by increasing the size of the holes in the outer rings [6-9]. These works indicate that between 4 and 9 rings of holes can be sufficient to reduce the confinement loss of dispersion flattened fibers to values close to the Rayleigh limit without significant compromise to the dispersion flatness, and various dispersion flattened fiber designs offering nonlinear parameters in the range 2 to $44 \text{ W}^{-1} \cdot \text{km}^{-1}$ have been proposed.

These theoretical papers have been primarily concerned with establishing designs that provide flat dispersion and low confinement loss, and no consideration has been paid to the fabrication precision required in order to obtain the desired dispersion behavior. However, it has been demonstrated both experimentally [4], and theoretically [10], that small deviations from the target design due to fabrication inaccuracies for even the simplest structures (i.e. a triangular lattice, with uniform hole size throughout the cladding) can lead to a significant deviation from

the anticipated dispersion properties. Understanding the sensitivity of the dispersion parameters to fabrication errors for different structural designs is thus an important issue

In this paper we apply a Genetic Algorithm [11] to the optimization of the dispersion of some of the NL-DFHF fibers already presented, and we demonstrate the effectiveness of our implementation in solving the inverse problem, as compared to the time consuming test-and-trial approach used so far to design such fibers. We then assess the typical statistical errors in both hole dimension and hole positions for a range of recently fabricated fibers to establish the current structural accuracy within holey fibers produced using the stack and draw technique, and analyze the sensitivity of the dispersion of such fibers to fabrication errors. This allows us to deduce some general guidelines for obtaining the desired dispersion characteristics.

2. Direct and inverse simulation methods

In order to calculate the wavelength dependence of the refractive index with the high accuracy required for chromatic dispersion calculations, we employ Femlab, a commercial full-vector mode solver based on the Finite Element Method (FEM). Anisotropic perfectly-matched layers (PML) [6] are positioned outside the outermost ring of holes in order to reduce the simulation window and to evaluate the confinement loss of HF with a finite number of rings of holes. The material dispersion is directly included in the calculations through the Sellmeier equation. We checked the accuracy of this method against the multipole method [12] for the case of a single ring structure with $\Lambda = 6.75 \mu\text{m}$ and $d = 5 \mu\text{m}$ at a wavelength of $1.45 \mu\text{m}$, and we obtained a good agreement in terms of calculated effective index (up to the fifth and ninth significant digit for the real and imaginary part respectively). We also compared the accuracy of our dispersion calculations by comparing our results with previously published FEM-based results for a 5 ring fiber with different hole sizes for each ring [6]. Agreement to within ± 0.3 ps/nm/km at all wavelengths between 1.2 and $1.8 \mu\text{m}$ was obtained.

As well as being accurate the FEM approach is relatively quick, allowing the full calculation of a dispersion curve within a few minutes on a standard PC for most of the NL-DFHF designs considered here. This calculation speed opens up the possibility of employing an inverse technique for the search of the optimal structure for a given specified characteristic, or indeed combination of characteristics. Although test and trial approaches based on simplified analytic assumptions can be effective for simple structures with a small number of free-parameters [3, 4] such approaches become impractical as the number of free design parameters is increased, e.g. by introducing a different hole size for each ring of holes. Moreover, the manual optimization of one parameter at a time can produce a sub-optimum answer. We therefore chose to implement a Genetic Algorithm (GA) for the inverse study of different NL-DFHF structures. The GA [13] is a generic optimization tool capable of simultaneously optimizing several parameters, and it has already been successfully applied to several inverse electromagnetic problems (see, for example Ref. [14]), and to the inverse design of constant hole size, dispersion flat HF [11]. The class of fibers that we currently restrict our study to are shown in Fig. 1: F1 and F2 are a 4 and 5 ring structure respectively in which the outer holes are kept large to improve the confinement loss, while the inner hole size is scaled down in order to control the dispersion profile (following the approach in Ref. [6]). Fiber F3 is a 5 ring fiber with a similar structure to the one proposed in Ref. [9], where the holes within the three internal and two outermost rings are of the same size, thereby reducing the fabrication complexity whilst preserving a flat dispersion curve.

Dispersion plays an important role in the performance of a nonlinear fiber, as it directly affects pulse broadening, walk-off and phase-matching conditions, thereby determining the bandwidth and power requirement of the device in which the fiber will be employed. For most telecoms applications a zero dispersion wavelength around 1550 nm is desirable, with a dispersion magnitude and slope designed to be as small as is possible. We target the dispersion

optimization by defining a fitness function F , used to evaluate the ‘quality’ of a given structure and minimized by the algorithm, as

$$F = \sum_{\lambda_i=1.5\mu\text{m}}^{1.6\mu\text{m}} |D(\lambda_i)| \quad (1)$$

where D is the dispersion parameter calculated at a wavelength λ_i and the sum is performed over 5 (uniformly spaced) points in the interval. The free parameters (or the ‘genes’ of the algorithm) are the pitch of the triangular lattice, Λ , and the diameter d_i of the holes in the i -th ring. Despite not directly including the nonlinear coefficient into Equation (1), we ensure that the fibers resulting from the optimization have a large nonlinearity by limiting the range over which Λ is allowed to change to small values (0.5-2.5 μm). By also applying a second restriction on the size of the holes in the outer ring (between 0.7 and 0.9 times Λ) we ensure at the same time a tighter mode confinement and a smaller confinement loss for the resulting fibers.

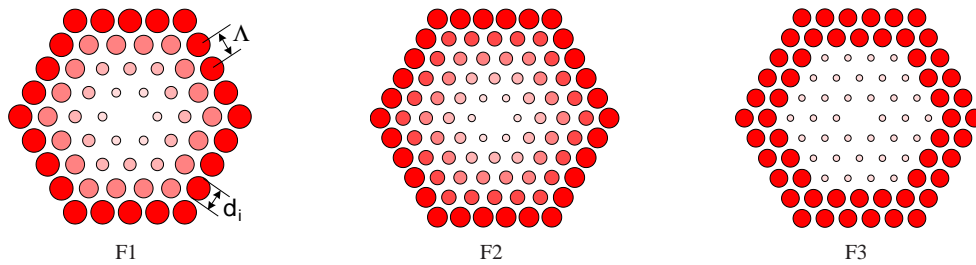


Fig. 1. Fiber structures to be optimized by the GA.

All the simulations were conducted on an initial population of 30 individuals, randomly chosen at the beginning of the computation. Convergence in the output fiber design specification was generally observed after 15 to 25 generations and took between 12 and 20 hours of computation time on a dual-processor Athlon MP-1200 machine. Randomly controlled processes of selection, crossover and mutation were implemented between each generation [13].

3. Optimized fibers

The structural parameters of the best fibers of each type, obtained through GA simulations are reported in Table 1. The effective area (A_{eff}) and confinement loss (CL) (for which the definitions in Ref. [6] have been used), calculated at 1.6 μm are also reported. We have also included, for means of comparison, the details of a fourth type of fiber, F4, which has equal sized holes throughout the structure. We did not need to use a GA to optimize this design since only 2 free parameters need to be optimized (Λ and d). We iterated to a 11-ring design that was close to that previously reported in Ref. [4]. The optimized dispersion curves for the 4 fibers are shown in Fig. 2.

A very flat dispersion behavior with a dispersion parameter D between ± 0.1 ps/nm/km across the wavelength range of interest is found for all 4 fiber types. The dispersion slopes of all fibers are less than 3×10^{-3} ps/nm²/km across the full 1.5 - 1.6 μm range considered, and remain below 1×10^{-3} ps/nm²/km for more than 50 nm around the central wavelength. Refinement of the objective function in order to minimize the slope itself rather than the total magnitude of dispersion across a given wavelength range should permit for even lower slopes about specific wavelengths in the C-band. As previously stated a primary advantage of using

Table 1. Structural parameters and optical properties of the best fibers obtained through the GA

Fiber	Λ [μm]	d_1/Λ	d_2/Λ	d_3/Λ	d_4/Λ	d_5/Λ	A_{eff} [μm^2]	CL [dB/m]
F1	1.567	0.323	0.450	0.693	0.853	-	8.75	$3.8 \cdot 10^{-3}$
F2	1.516	0.317	0.484	0.571	0.632	0.667	8.3	$1.1 \cdot 10^{-4}$
F3	2.133	0.281	0.281	0.281	0.767	0.767	21.9	$1.6 \cdot 10^{-5}$
F4	2.406	0.251	0.251	0.251	0.251	0.251	38.7	$6.5 \cdot 10^{-1}$

the GA approach is that these structures were determined in a fully automated manner in a time of between 12 and 20 hours rather than using the laborious manual test and trial approaches originally used to iterate to these general forms of structure.

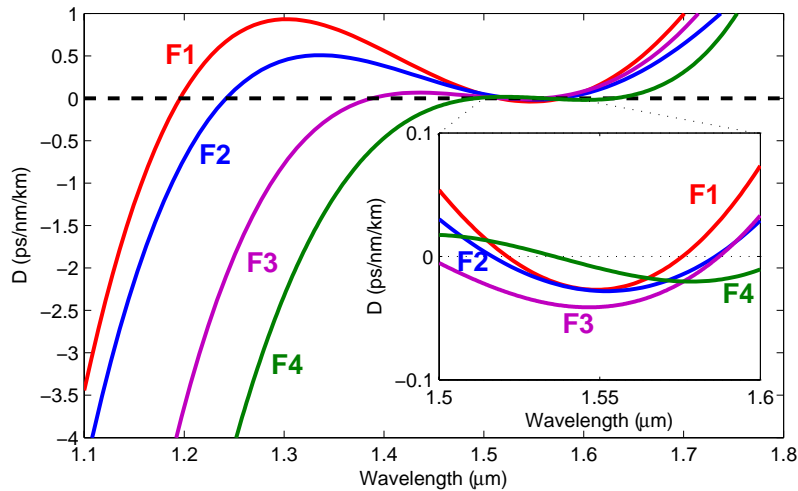


Fig. 2. Solutions of the Genetic Algorithm for the 3 fibers in Fig. 1. Plot F4 is the dispersion of an 11 rings structure with constant d/Λ for all the holes. The inset zooms on the wavelength range in which the fibers have been optimized

Despite a similar dispersive behavior in the region of interest, evident differences can be seen in terms of A_{eff} and CL. Fibers F1 and F2 offer a higher nonlinear coefficient [$\gamma = (2\pi n_2)/(\lambda \cdot A_{eff})$] whereas fiber F3 presents the best confinement loss. The simplest structure, fiber F4, despite showing the flattest behavior, exhibits the worst characteristics in terms of both nonlinearity and confinement loss, and from simulations, an impractical number of more than 15 rings of holes would be required in order to reduce the confinement loss to a level similar to fiber F3. However we note that of all the fibers considered only fiber F4 is rigorously single mode: fibers F1-F3 all theoretically present higher order modes that are localized between the innermost two rings of holes. The higher confinement loss of these modes and the large difference in effective index between them and the fundamental mode suggests though that these fibers are likely to be effectively single mode in practice [8]. Note for completeness that the splice loss to SMF is likely to be more significant for fibers F1 and F2 than F3 and F4 due to the larger mode mismatch.

4. Practical fabrication considerations

Having demonstrated that fibers with exceptional flatness in a 100 nm range around 1550 nm can be theoretically realized using various different design approaches, we went on to investigate how the inevitable imprecision introduced during the fabrication process affects the final dispersion profile. Before doing this, in order to inform our calculations, we decided to establish the accuracy that we are currently able to achieve in terms of hole size definition and positioning using our current stack and draw procedures. To do this we took Scanning Electron Micrographs (SEMs) of three fibers recently produced at our facility and measured the hole diameter and shift from their target position on a hexagonal lattice for the 2 innermost rings of air holes. These air holes have the largest influence on both the nonlinear and dispersive properties of the fiber. Two of the fibers were large mode area (LMA-) HF designs and the third a small-core, high-nonlinearity (HNL-) HF design. The results are summarized in Table 2, where we use the standard-deviation to average diameter ratio as our measure of accuracy in hole size, and the mean absolute off-centeredness over the average pitch (θ_{pos}) as our measure of precision in the hole position:

Table 2. Fabrication tolerances for a range of structurally different fibers

Fiber	Λ_{avg} [μm]	Hole diameters				θ_{pos}	
		d_{avg} [μm]	d_{min} [μm]	d_{max} [μm]	st. dev. / d_{avg}	Ring 1	Ring 2
LMA-1	11.37	2.33	2.21	2.60	4%	2.4%	3.9%
LMA-2	7.65	3.79	3.65	4.09	3%	2.0%	2.6%
HNL-1	1.93	0.80	0.76	0.85	2%	2.2%	3.7%

It is interesting to note that despite the large difference in terms of hole size and pitch between the two forms of fiber, the overall percentage discrepancies from the target values are all very similar. The hole size can be defined to a level of between 2 and 4% of the average value. The mean absolute distance between the holes and their optimum position in the triangular lattice was defined to a value of between 2 and 2.4% of Λ for the first ring of holes, increasing slightly to around 3-4% for the second ring.

In order to understand how this level of imprecision in fabrication manifests itself in terms of the overall dispersion behavior we have run a set of simulations on all 4 fiber types, in which we modified Λ and d/Λ for each ring of holes by $\pm 1\%$, $\pm 2\%$, $\pm 5\%$ and $\pm 10\%$ from the optimum value. Note that this study serves to provide an upper bound on the severity of the fabrication imperfections, because in reality not all the holes are distorted from their optimum value or position in the same way, and some averaging effect is likely to occur. Results for fiber F2, presented in Fig. 3, permit us to deduce the following general rules which are also valid for the other fibers studied:

- In the case of an already flat dispersion, an error in the pitch dimension mainly results in a shift towards a higher or lower value of the dispersion parameter. This can be used to achieve a slightly normal or anomalous flat dispersion from the same stacked preform or cane.
- The dimension of the first ring represents the main contribution to the overall dispersion slope, and particular care must be applied to try and match the optimum value, if a flat behavior is required. Also it can be observed that an increase of d_1 causes the dispersion

parameter to decrease, the opposite behavior is observed for all the other rings. This has previously been observed in Ref. [7] and is further evidenced by the fact that HF for dispersion compensation needs a large air fill fraction for the first ring of holes.

- The overall contribution of the second ring to the total dispersion is still large, but it has less effect on the slope. An error in the dimension of the second ring of holes can be compensated through an overall scaling of the structure.
- The influence of the third ring of holes is more limited and, although not shown here, the contribution from the fourth and fifth rings is almost negligible. This suggests that for this fiber the holes in these rings can be designed with as large a d/Λ as desired to reduce the confinement losses.

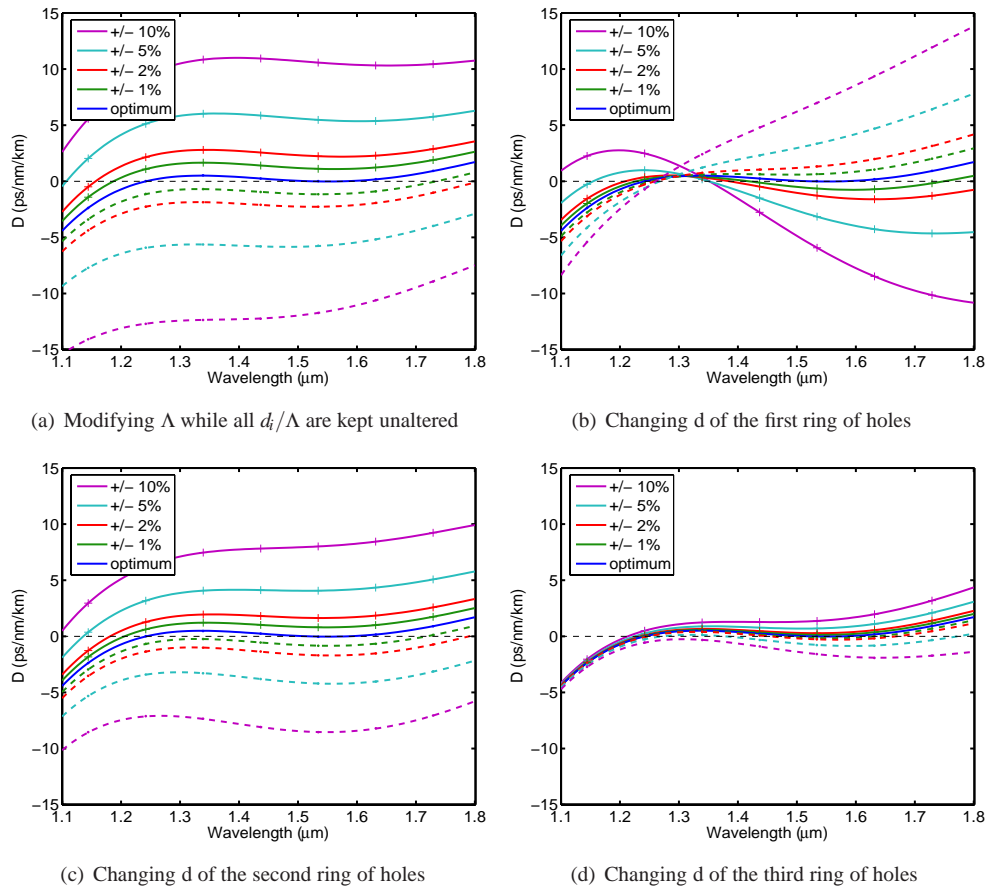


Fig. 3. Variation of the total dispersion profile as some structural parameters are changed for fiber F2. Dotted lines indicate a '-' variation, while continuous lines represent a '+' variation.

Figure 4 represents the effect of modifying the radius of an entire ring while the rest of the structure is unaltered. We experimentally found that, while this occurrence is very rare in the fabrication of fibers with equal hole sizes, it can easily happen during the pulling of fibers with different d/Λ per ring due to the different forces that each capillary is then subjected to due to

pressure and surface tension. Figure 4(a) shows that the detrimental effect of inaccuracy in the position of air holes in the first ring is even more severe than an inaccuracy in the hole size, and that off-centredness of the holes can cause significant modifications to the overall dispersion profile. Errors in the position of the second ring of holes also produce large undesirable effect. Effects within the third ring onwards are small and progressively less significant.

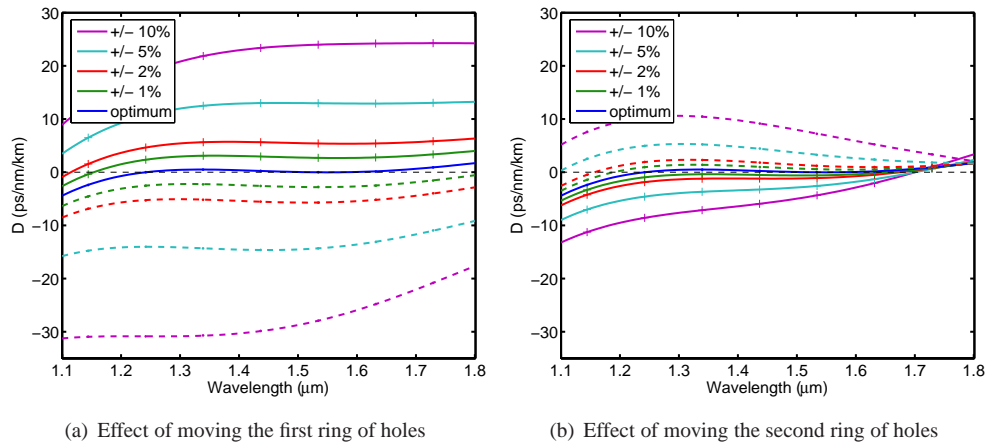


Fig. 4. Variation of the total dispersion profile as all the holes in a ring are displaced from optimum position for fiber F2. Dotted lines indicate a '-' variation, while continuous lines represent a '+' variation.

A similar qualitative behavior to that shown in Fig. 3 and 4 for fiber F2 was also observed for the other fiber types, albeit with different magnitudes. To complete the analysis we present, in Fig. 5, a sensitivity comparison between fibers F1-F4 to a change in d_1 , which, as shown in Fig. 3 is the most critical parameter as far as dispersion flatness is concerned. We have plotted the average dispersion parameter $D_{average} = (D_{1.5\mu m} + D_{1.6\mu m})/2$ and the average dispersion slope $D_{slope} = (D_{1.6\mu m} - D_{1.5\mu m})/100nm$ for all the fibers as d_1 is either increased or decreased from its optimum calculated value. From both figures it is evident that structure F3 is generally the least sensitive to structural variations. Fiber F4 is also less sensitive to perturbations than fibers F1 and F2, other than for large positive errors which cause large negative dispersion shifts from the optimum. Fibers F1 and F2 exhibit similar behavior, and are almost a factor of 2 more sensitive to fabrication errors than fiber F3. Their overall slope is also the most sensitive to imperfections of this type. Figure 5(b) also shows very clearly that in order to achieve the theoretically predicted ultra-low slopes of less than 10^{-3} ps/nm²/km a precision of less than 1% has to be reached in the size of the first ring of holes with these types of NL-DFHF.

5. Discussion and conclusions

We have applied, for the first time to our knowledge, a GA to the inverse design of HF with a large number of free parameters (up to 6) and for which the manual optimization approach becomes unreliable and cumbersome.

The chosen design goal was a holey fiber with flat and nearly zero dispersion characteristics over a 100 nm range centered at $1.55 \mu m$, and our approach has proved effective in finding various optimized solutions with $D = 0 \pm 0.1$ ps/nm/km over the full wavelength range of interest. Despite possessing similar dispersion characteristics, the fibers analyzed present different non-linear coefficients, ranging from $2.2 W^{-1} \cdot km^{-1}$ for fiber F4 to $10.4 W^{-1} \cdot km^{-1}$ for fiber F2. Fiber F3, representing a structural compromise between holes with the same size throughout

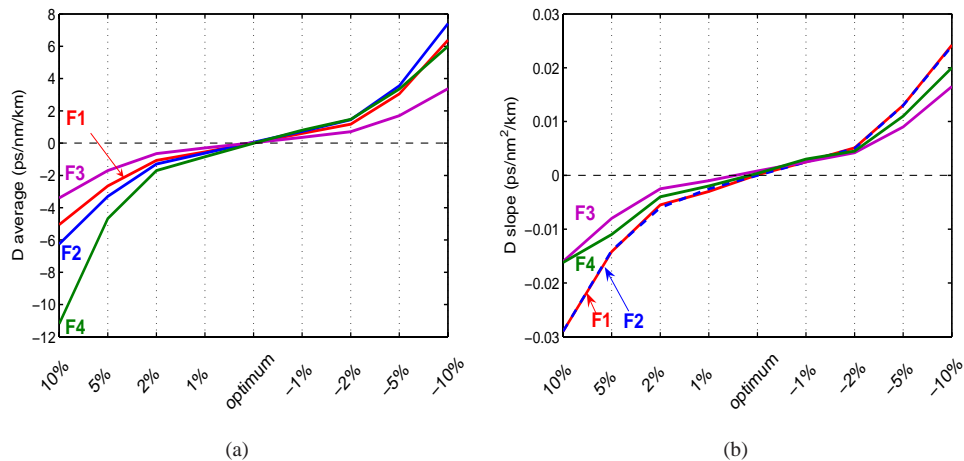


Fig. 5. Sensitivity of the 4 fibers to an error on the dimension of the first ring of air holes: (a) average dispersion parameter and (b) dispersion slope in the interval 1.5 - 1.6 μm .

the cladding and different hole sizes for each ring, offers an intermediate nonlinear coefficient ($\gamma = 3.9 \text{W}^{-1} \cdot \text{km}^{-1}$). Similar values of dispersion slope and nonlinear coefficient to those provided by the 4 NL-DFHF analyzed here have also recently been achieved in conventional doped fibers [1] although it is to be appreciated that the fabrication tolerances are extremely demanding. Moreover it is well known that the higher index contrast of HF can lead to the realization of fibers with a larger nonlinear coefficient than is achievable with conventional fibers. Silica NL-DFHF with a nonlinear coefficient as high as $44 \text{W}^{-1} \cdot \text{km}^{-1}$ and slightly compromised slope have already been identified and simulated [7], and can be targeted more systematically in the future by extending the generic approach demonstrated in this paper. Future work can be addressed, through the definition of different fitness functions, to the maximization of the nonlinear coefficient of NL-DFHF, or to select the structure providing the highest proposed figure-of-merit for short length nonlinear devices [15]. Other useful design goals can also be targeted such as flattened dispersion at wavelengths around $1 \mu\text{m}$, or a dispersion characteristic with two specifically positioned zero-dispersion wavelengths [16].

Fabrication guidelines for the structures established in this paper have also been proposed, indicating that the dimension of the first ring of holes is particularly important in controlling the dispersion flatness. It is also important to accurately define the pitch, the dimension of the holes in the second ring of holes, and the position of the first two rings of holes. We have found that some geometries, like F3, beside presenting an easier fabrication target than fibers F1 and F2, are also nearly twice less sensitive to fabrication errors - albeit with reduced fiber nonlinearity. From the analysis presented, we can roughly estimate that an accuracy of order 1-2% will be required for most of the critical structural parameters in order to control the overall dispersion with reasonable accuracy. Measurements on some of our recently fabricated fibers indicate that such a level of accuracy is well within sight and should be achievable with realistic improvements in the preform fabrication and fiber drawing processes.

Acknowledgments

T. M. Monro gratefully acknowledges the support of the Royal Society through a University Research Fellowship. Her current address is: School of Chemistry & Physics, University of Adelaide, Adelaide SA 5005, Australia.